

12. Shultz, J. W. & Regier, J. C. Phylogenetic analysis of arthropods using two nuclear protein-encoding genes supports a crustacean + hexapod clade. *Proc. R. Soc. Lond. B* **267**, 1011–1019 (2000).
13. Boore, J. L., Lavrow, D. V. & Brown, W. M. Gene translocation links insects and crustaceans. *Nature* **392**, 667–668 (1998).
14. Dohle, W. Are the insects terrestrial crustaceans? A discussion of some new facts and arguments and the proposal of the proper name 'Tetraconata' for the monophyletic unit Crustacea + Hexapoda. *Ann. Soc. Entomol. France* **37**, 85–103 (2001).
15. Strausfeld, N. J. Crustacean–insect relationships: The use of brain characters to derive phylogeny amongst segmented invertebrates. *Brain Behav. Evol.* **52**, 186–206 (1998).
16. Wheeler, W. C. Optimization alignment: The end of multiple sequence alignment in phylogenetics? *Cladistics* **12**, 1–9 (1996).
17. Wheeler, W. C. & Gladstein, D. POY (2000). Program and documentation available at <ftp://amnh.org/pub/molecular>.
18. Gee, H. Homegrown computer roots out phylogenetic networks. *Nature* **404**, 214 (2000).
19. Zrzavý, J. & Štys, P. The basic body plan of arthropods: Insights from evolutionary morphology and developmental biology. *J. Evol. Biol.* **10**, 353–367 (1997).
20. Zrzavý, J., Hypša, V. & Vlaskova, M. *Arthropod Relationships* (eds Fortey, R. A. & Thomas, R. H.) 97–107 (Chapman & Hall, London, 1998).
21. Regier, J. C. & Shultz, J. W. Molecular phylogeny of the major arthropod groups indicates polyphyly of crustaceans and a new hypothesis for the origin of hexapods. *Mol. Biol. Evol.* **14**, 902–913 (1997).
22. Colgan, D. J. *et al.* Histone H3 and U2 snRNA DNA sequences and arthropod molecular evolution. *Aust. J. Zool.* **46**, 419–437 (1998).
23. Kluge, A. G. A concern for evidence and a phylogenetic hypothesis of relationships among *Epicrates* (Boidae, Serpentes). *Syst. Zool.* **38**, 7–25 (1989).
24. Wheeler, W. C. Sequence alignment, parameter sensitivity, and the phylogenetic analysis of molecular data. *Syst. Biol.* **44**, 321–331 (1995).
25. Spears, T. & Abele, L. G. *Arthropod Relationships* (eds Fortey, R. A. & Thomas, R. H.) 169–187 (Chapman & Hall, London, 1998).
26. Goloboff, P. A. NONA v. 2.0 (1998). Program and documentation available at <ftp://unt.edu.ar/pub/parsimony>.
27. Wahlberg, N. & Zimmermann, M. Pattern of phylogenetic relationships among members of the tribe Melitaeini (Lepidoptera: Nymphalidae). *Cladistics* **16**, 347–363 (2000).
28. Bremer, K. The limits of amino acid sequence data in angiosperm phylogenetic reconstruction. *Evolution* **42**, 795–803 (1988).
29. Goloboff, P. A. Analyzing large data sets in reasonable times: Solutions for composite optima. *Cladistics* **15**, 415–428 (1999).
30. Farris, J. S., Källersjö, M., Kluge, A. G. & Bult, C. Constructing a significance test for incongruence. *Syst. Biol.* **44**, 570–572 (1995).

Supplementary information is available on Nature's World-Wide Web site (<http://www.nature.com>) or as paper copy from the London editorial office of Nature.

**Acknowledgements**

We thank all those who have assisted us with morphological discussions, laboratory work (especially K. Demeo), collecting specimens, and given any other form of help or advice. D. Colgan and G. Wilson have been valued collaborators. S. Thurston provided technical illustration. J. Shultz and L. Prendini shared specimens and unpublished sequence data. Funding was mainly provided by the Fundamental Biology Program of NASA.

Correspondence and requests for materials should be addressed to G.G. (e-mail: [ggiribet@oeb.harvard.edu](mailto:ggiribet@oeb.harvard.edu)). GenBank accession codes for the new sequences are AF370781–AF370876.

**Dissociation between hand motion and population vectors from neural activity in motor cortex**

**Stephen H. Scott, Paul L. Gribble\*, Kirsten M. Graham & D. William Cabel**

CIHR Group in Sensory-Motor Systems, Centre for Neuroscience Studies, Department of Anatomy and Cell Biology, Queen's University, Kingston, Ontario K7L 3N6, Canada

The population vector hypothesis was introduced almost twenty years ago to illustrate that a population vector constructed from neural activity in primary motor cortex (MI) of non-human primates could predict the direction of hand movement during reaching<sup>1–6</sup>. Alternative explanations for this population signal

have been suggested<sup>7,8</sup> but could not be tested experimentally owing to movement complexity in the standard reaching model. We re-examined this issue by recording the activity of neurons in contralateral MI of monkeys while they made reaching movements with their right arms oriented in the horizontal plane—where the mechanics of limb motion are measurable and anisotropic. Here we found systematic biases between the population vector and the direction of hand movement. These errors were attributed to a non-uniform distribution of preferred directions of neurons and the non-uniformity covaried with peak joint power at the shoulder and elbow. These observations contradict the population vector hypothesis and show that non-human primates are capable of generating reaching movements to spatial targets even though population vectors based on MI activity do not point in the direction of hand motion.

Primary motor cortex (MI) has an important function in controlling visually guided limb movements, and a central problem in motor research has been to identify how neurons within MI participate in these tasks<sup>4,9</sup>. Several studies have shown that the activity of individual neurons is sensitive to many different parameters related to target, hand and limb movement<sup>5,10–13</sup>. However, it has been shown that if individual cells are represented as vectors, with direction defined by the cell's preferred direction (PD), the direction of movement in which the cell is maximally active) and magnitude defined as the cell's discharge rate for a given movement direction, the resulting vector sum (population vector) of all cell vectors is congruent with the direction of hand movement<sup>1–3,6</sup>. This ability to predict hand motion has supported the idea that MI may reflect a higher level representation related to movement direction<sup>4,5</sup>. Theoretical studies, however, have argued that neural activity in myriad coordinate frames related to sensory or motor features of the task would also produce population vectors that point in the direction of hand motion<sup>7,8,14</sup>. This debate on the neural representation of movement in MI is important not only for understanding its role in movement planning and control, but also for understanding the computational processes performed by other regions of the central nervous system, such as the spinal cord. Although some deviations between the population vector and hand motion have been observed<sup>15</sup>, they have been small and difficult to interpret.

Considerable insight into human motor performance and learning has been gained from studies of planar limb movement where the arm is oriented in the horizontal plane, hand motion is generated only by flexion and extension motions at the shoulder and elbow, and the mechanics of movement can be easily estimated<sup>16–21</sup>. The mechanics of these planar movements are anisotropic with large variations that are dependent on movement direction<sup>17</sup>. We addressed whether the activity of MI neurons at the population level was influenced by these mechanical anisotropies.

We trained monkeys to make planar movements with roughly straight hand trajectories to spatial targets (Fig. 1a). We recorded the activity of neurons in the left contralateral MI of monkeys while they made reaching movements with their right hand from a central target to eight spatial targets that were located on the circumference of a circle. The activity of 214 neurons was found to be unimodally tuned to the direction of movement (62, 22 and 130 in monkeys *a*, *b* and *c*, respectively). As shown previously, cell activity was broadly tuned to the direction of movement. Figure 1b shows the activity of a typical cell in MI during the task where maximal activity occurred when the monkey moved its hand to the right and towards itself (PD = 326°).

We constructed population vectors from our cell sample and compared these vectors to the actual directions of hand motion. Population vectors during movement tended to be biased towards one of two directions: away and left, or towards and right (Fig. 2a). Thirteen of the 16 population vectors did not point in the direction of hand motion (Fig. 2b). There was no significant correlation

\* Present address: Department of Psychology, The University of Western Ontario, London, Ontario N6A 5C2, Canada.

between deviations in the population vector and deviations in hand movement relative to target direction ( $r^2 = 0.07$ ;  $P > 0.05$ ). Furthermore, there were large fluctuations in population vector length, varying from 56 to 145% of the mean value across all directions. This modulation of the magnitude of the population vector occurred despite the fact that hand movements were of similar magnitude.

Population vectors will tend to point in the direction of movement if certain conditions are met: no coupling between a cell's PD and the magnitude of its tuning, and a uniform distribution of PDs<sup>7,14</sup>. We examined the former condition by comparing cell modulation against PD. Cell modulation was defined as the highest mean discharge rate before and during movement (reaction time (RT) + movement time (MT)) measured for any movement direction minus its lowest mean discharge rate for any movement direction. Mean cell modulation for a given movement direction was defined from all cells with PDs within  $\pm 22.5^\circ$  of that direction. We found no significant correlation between peak joint power and mean cell modulation associated with each movement direction. ( $r^2 = 0.04$ ;  $P > 0.05$ ; see Supplementary Information).

We examined the distribution of PDs for our sample by segregating cells into 16 groups on the basis of their PD (bin size =  $22.5^\circ$ ) and

then plotting the numbers of cells in each bin against movement direction (Fig. 3a). Spatial directions were not equally represented across the cell sample and the distribution of PDs was found not to be uniform, particularly when compared against a bimodal distribution (bimodal distribution,  $P < 10^{-5}$ , main axis =  $117\text{--}297^\circ$ ; unimodal distribution,  $P < 0.01$ , mean vector is  $26^\circ$ , Rayleigh test). There were two apparent clusters, one for movements away and left, and another for movements towards and right. Cells recorded in each individual monkey showed similar biases in their distribution

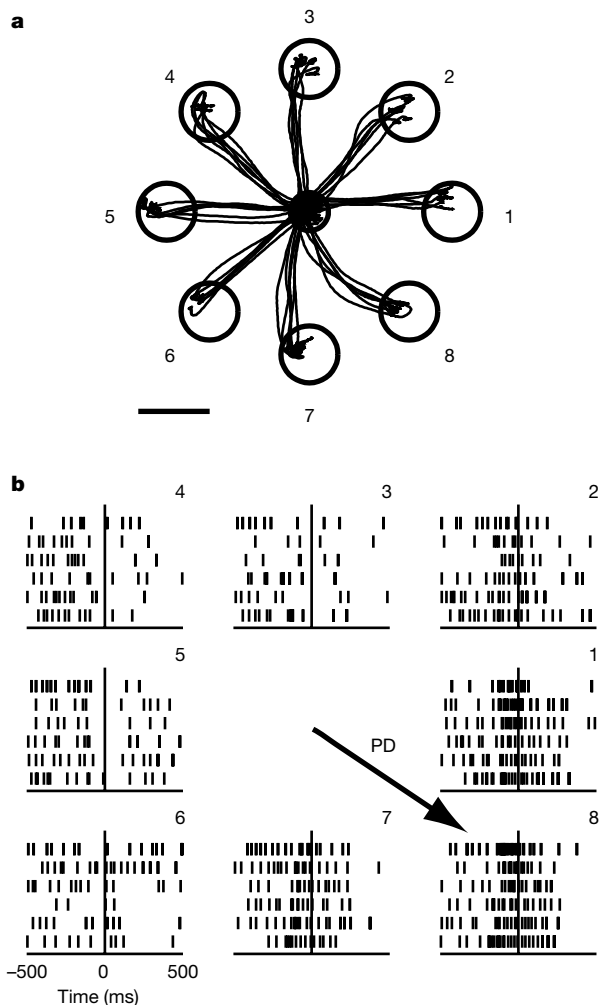


**Figure 1** Cell activity in primary motor cortex (MI) during reaching. **a**, Hand trajectory for six repeat trials to eight spatial targets. Scale bar, 3 cm. **b**, Corresponding neural activity for each movement. Each raster plot shows the discharge pattern of the cell for six repeat trials where each small vertical line denotes the occurrence of an action potential. Long vertical bars denote movement onset. The arrow defines the cell's preferred direction (PD), the direction in which it is maximally active (PD =  $326^\circ$ ).

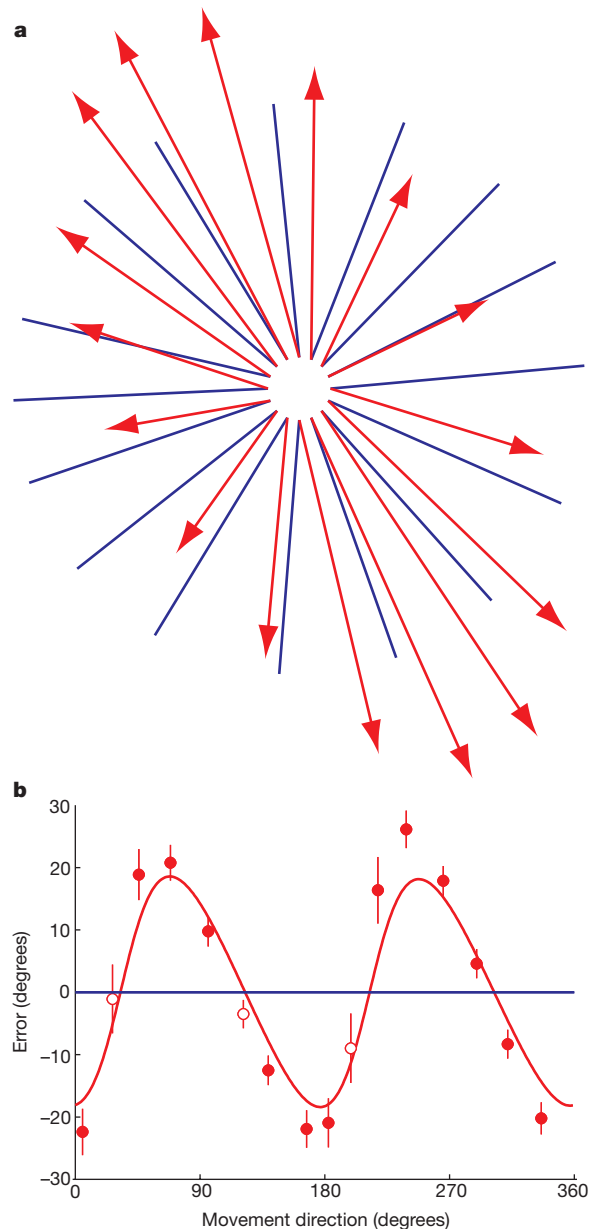


**Figure 2** Comparison between population vectors and directions of hand movement. **a**, The base of each population vector (red arrow) is attached to the corresponding direction of hand movement (blue line). **b**, Difference between the direction of population vector and the direction of hand movement. Filled circles denote significant differences between the population vector and movement direction at the 1% level; open circles denote no significant difference ( $P > 0.01$ ). The vertical line through each circle represents 1 s.d. in the distribution of re-sampled population vectors (see Methods). The thick red line denotes a theoretical prediction of population vector error for all movement directions on the basis of a simulated population of 1,000 cells with a bimodal distribution similar to that observed in the present study where the tuning of each cell was based on a unimodal von Mises function.

of PDs (Fig. 3c–e). Afferent feedback cannot account for these results as a similar non-uniform distribution was observed when the directional preference of cells was based only on their activity during the reaction time period (Fig. 3b; bimodal distribution,  $P < 10^{-5}$ , main axis = 118–298°,  $n = 141$ ; only cells tuned during RT included in this distribution).

Variations in the distribution of PDs were compared to several different kinematic and kinetic features of movement. Hand velocity was essentially the same for movements in the different spatial directions and did not correlate with the distribution of PDs ( $r^2 = 0.10$ ; Fig. 4a). Peak joint velocity (sum of shoulder and elbow joint velocity) varied for movements in different spatial directions and showed a modest correlation with the distribution of PDs ( $r^2 = 0.54$ ; Fig. 4b). Although peak joint torque varied with movement direction, it did not correlate at all with the distribution of PDs ( $r^2 = 0.002$ ; Fig. 4c).

Joint power is a variable that characterizes the mechanical characteristics of the limb as it incorporates two important features of the peripheral motor apparatus: joint torque, which reflects the anisotropic inertial properties of the limb<sup>17</sup>, and joint velocity, which reflects muscle force reduction with shortening velocity<sup>22</sup>. Figure 4d shows that peak joint power varies strongly for movements in different spatial directions. Peak power for movements of the right arm tends to be larger for movements away and to the left (upper left quadrant), and for movements towards and to the right (lower right quadrant). Notably, variations in the distribution of PDs paralleled the anisotropy in peak joint power (Fig. 4d). Movement directions requiring larger peak joint power tended to have more directionally tuned cells than directions requiring less power. A statistically significant correlation ( $r^2 = 0.76$ ) was found between joint power and cell counts associated with each movement direction ( $P < 0.01$ ). Moreover, variations in the length of population vectors for different movement directions correlated strongly with

peak joint power ( $r^2 = 0.94$ ;  $P < 0.001$ ).

The distribution of PDs is somewhat non-uniform when reaching movements are performed with the shoulder near a neutral abduction/adduction angle, but becomes more skewed when reaching with the shoulder abducted at an angle of about 80° (ref. 11). As compared with ref. 11, we found an even stronger non-uniformity when the shoulder was abducted 90° and the arm was maintained in the horizontal plane during reaching. The smaller non-uniformity found in this previous study was probably a result of the arm not being entirely restricted to the horizontal plane and that the

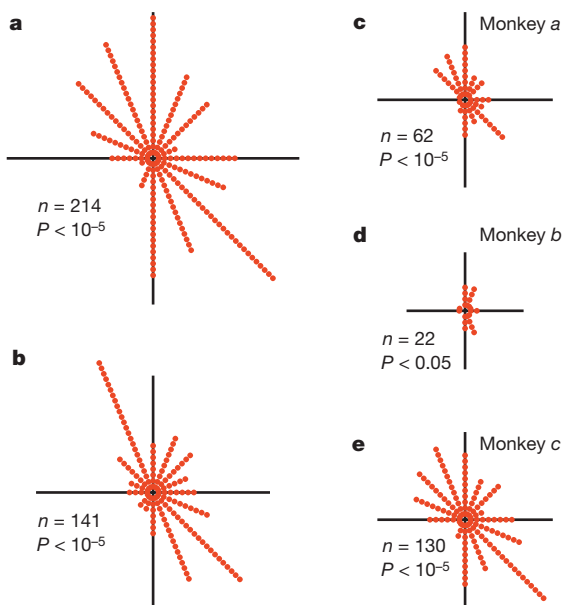


**Figure 3** Directional preference of cells in MI. **a**, Distribution of PDs for the 214 directionally tuned cells during reaction time + movement time (RT + MT) recorded in contralateral motor cortex during movements of the right hand. Each circle represents the directional preference of an individual cell and cells are grouped into 16 equal-sized bins (bin size = 22.5°). The  $P$ -value in the panel reflects the statistical level at which the distribution was found to be non-uniform as compared with a bimodal distribution. **b**, Distribution of PDs on the basis of the activity of neurons during the reaction time period (300 ms before movement onset). Only neurons directionally tuned before movement onset were included in this sample. **c–e**, Distribution of PDs for neurons recorded in each individual monkey during RT + MT.

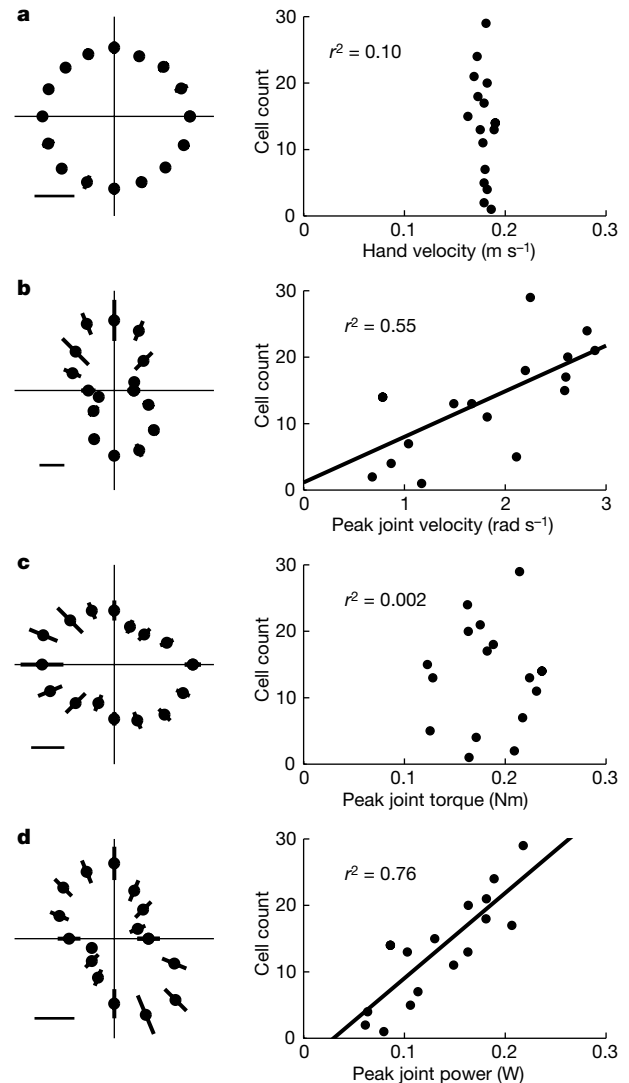


**Figure 4** Comparisons between distribution of PDs and various kinematic and kinetic features of movement. Kinesiological values based on all movements in which neural activity was recorded in this task. **a**, Left, polar plot of peak hand velocity relative to direction of hand movement for 16 targets uniformly distributed in space. Mean and s.d. are defined with filled circles and thick lines, respectively. Scale bar, 0.1 m s<sup>-1</sup>. Right, peak hand velocity for a given movement direction plotted against the number of neurons with PDs within ± 11.25° of each movement direction. **b**, Variations in peak joint velocity (sum of shoulder and elbow) for movements in different spatial directions. Scale bar, 1 rad s<sup>-1</sup>. Right panel illustrates a significant correlation between joint velocity and cells associated with that direction of movement ( $P < 0.01$ ; black line denotes regression line). **c**, Left, variations in peak joint torque for movements in different directions. Right, lack of a correlation between joint torque and cell counts for each movement direction. Scale bar, 0.1 Nm. **d**, Polar plot of peak joint power relative to direction of hand movement. Scale bar, 0.1 W. Right, significant correlation between joint power and the distribution of PDs ( $P < 0.01$ ). Variations in peak joint power can explain 76% of the variability in the distribution of PDs.

monkeys moved a pendulum, which requires larger shoulder torques in the frontal as compared with the sagittal plane. Although it is difficult to identify exactly why there is a difference in the distribution of PDs between studies, the non-uniformity observed with the shoulder abducted 90° probably reflects several interacting factors. First, limb mechanics are highly anisotropic. Second, hand movements are generated only by flexion and extension motions at the shoulder and elbow rather than including other degrees of freedom at the shoulder. Third, our previous study, where muscular torque is systematically manipulated during posture, shows that proximal forelimb muscles and neuronal activity in MI tend to be preferentially related to flexor torque at one joint combined with extensor torque at the other<sup>23</sup>. This multi-joint coupling would tend to generate a greater non-uniformity in the distribution of PDs during this reaching task than predicted if neurons were randomly associated to muscle groups at each joint.

A central advance in our study was that the distribution of PDs was correlated to mechanical anisotropies. This correlation suggests that the role of MI in compensating for the mechanical properties of the limb overrides any requirement to maintain a uniform distribution of PDs related to the direction of hand movement. As a result we found that a vector constructed from the ensemble activity of neurons in MI, as described by the population vector hypothesis, does not have to point in the direction of movement for non-human primates to successfully move their hands to spatial targets. Of course, hand motion may be computed from this population of cells either by selecting a sub-population of cells from our sample that are uniformly distributed, or by using more complex computational strategies rather than the population vector method<sup>24,25</sup>.

The success of joint power to predict the distribution of PDs may be partially due to the fact that it is a first approximation of muscle activation during reaching. Muscle activation reflects not only force (or torque) but also velocity as force production drops markedly with muscle shortening velocity<sup>22</sup>. Maximal activities of shoulder and elbow muscles were similar to that observed for MI cells (data not shown). We cannot easily separate these two variables in the present task, and the advantage of using joint power is that it can be easily computed from joint kinematics and inverse dynamics. It is important to note that the present results should not be construed as evidence that neural activity in MI explicitly codes joint power (or even muscle activation) because many variables influence cell activity<sup>5,10–13</sup>. However, this study does emphasize that the complex role played by MI in controlling multi-joint movements cannot be captured easily with a hand-based framework; further progress in this field will require peripheral-based paradigms that consider the mechanics of the limb. □

## Methods

### Experimental paradigm

Three male rhesus monkeys (6–7 kg) were trained to wear a mechanical exoskeleton that permitted flexion and extension motion of the shoulder and elbow joints in the horizontal plane<sup>26</sup>. Monkeys were trained to make movements from a central target (0.8 cm radius) to 16 peripheral targets (1.2 cm radius) uniformly distributed on the circumference of a circle (6 cm radius). A successful trial required the monkey to move between the spatial targets in 220–350 ms (shorter than overall movement time; see below). This movement criteria along with overtraining from months of practice probably resulted in constant movement times for all spatial directions (Fig. 4a), which contrasts with previous observations that hand velocity varies with movement direction in naive human subjects<sup>27</sup>. The monkey was fully trained to perform these movements consistently before neural recordings were initiated. All procedures followed university and national guidelines for animal care.

Recording chambers were implanted surgically under inhalation anaesthetic and we used conventional techniques for extracellular recording of single-neuron activity related to the proximal arm in MI (ref. 11). The territory where cell activity was sampled in MI was similar to the region examined in previous studies on reaching<sup>11</sup>. Neurons recorded in the task were located in the rostral bank and crown of the central sulcus where trains of electrical stimulation (11 pulses, 333 Hz, 0.2 ms pulse width, range 5–50  $\mu$ A) elicited movement of the shoulder or elbow. Cells were examined in the task if they were active during reaching and if they responded predominantly to passive movement of the shoulder and/or elbow. Cells that did not respond to passive movement of any of the forelimb joints were recorded in the task if neighbouring neurons responded only to

passive movement of the shoulder and/or elbow. Neuronal activity was collected along with a number of variables related to hand and joint motion using a custom-designed, data-acquisition system<sup>26</sup>. Cell activity was usually recorded in six repeat trials to 8 of the 16 targets that were presented in a pseudo-random block design. In the first two monkeys (*a* and *b*), neural activity was recorded for movements to 8 targets selected specifically to sample joint-based frameworks (45, 67.5, 90, 180, 247.5, 270, 305 and 327.5°, where 0° is to the right and positive rotation is anticlockwise). Most of the neurons recorded in this study are from monkey *c*, where neural activity was recorded for movements to 8 targets that were distributed symmetrically in space (0, 45, 90, 135, 180, 225, 270 and 315°).

### Data analyses

Mean movement time was 576 ms across all directions and movement onset was defined as 10% of peak hand velocity. Cell activity was based on the number of action potentials recorded 300 ms before movement onset to 575 ms after movement onset (RT + MT). Shoulder and elbow muscular torques were calculated using inverse dynamics<sup>26,28</sup>. Joint power was computed by multiplying each joint's muscular torque by its angular velocity<sup>29</sup> and summing these values for the shoulder and elbow together at 5 ms time intervals. Peak values for each variable equalled the largest summed value for each movement direction.

Most of the cells in this study were recorded from monkey *c* where movement directions were equally distributed in space. The directional preferences of these cells were estimated using standard trigonometric techniques where the directional bias of the cell was defined by a mean vector whose orientation defines the cell's preferred movement direction<sup>11,30</sup>. For neural data recorded in monkeys *a* and *b*, the spatial targets were distributed non-symmetrically. We adapted techniques to describe the area of planar objects to identify the cell's mean vector for each block of eight trials (see Supplementary Information). A standard bootstrap technique was used to define whether the directional tuning of each cell, as defined by the mean vector, was statistically significant at the 1% level<sup>11</sup>.

We tested whether the distribution of PDs was uniform as compared to either a unimodal or bimodal distribution. In each case, a mean vector was computed from the observed distribution of PDs and the statistical test identified whether a random sample drawn from a uniform distribution (all directions equally represented) could generate a vector of similar or greater length (statistics based on 1,000,000 repeat samples).

Population vectors were computed for the cell population using standard techniques<sup>3</sup>. As neural activity was recorded in only 8 of the 16 movement directions, von Mises tuning functions were used to characterize the activity of a cell for each movement direction relative to the mean discharge across directions (see Supplementary Information). We used a bootstrap method to identify whether the direction of each population vector was significantly different from the corresponding direction of hand motion<sup>31</sup>. The direction of hand motion for each target was defined by its position at peak hand velocity relative to its initial position before movement onset. For each movement, populations of 214 cells were re-sampled with replacement from the original distribution, and the population vector for each sample was computed to define a sampling distribution of population vectors for each movement direction (total re-sampled distributions = 1,000). The population vector was identified as significantly different from the direction of hand movement if less than 1% of the re-sampled distributions crossed mean hand direction.

Received 19 April; accepted 24 July 2001.

- Georgopoulos, A. P., Caminiti, R., Kalaska, J. F. & Massey, J. T. Spatial coding of movement: a hypothesis concerning the coding of movement directions by motor cortical populations. *Exp. Brain Res. (Suppl. 7)* 327–336 (1983).
- Georgopoulos, A. P., Schwartz, A. B. & Kettner, R. E. Neuronal population coding of movement direction. *Science* **233**, 1416–1419 (1986).
- Georgopoulos, A. P., Kettner, R. E. & Schwartz, A. B. Primate motor cortex and free arm movements to visual targets in three-dimensional space. II. Coding of the direction of arm movement by a neural population. *J. Neurosci.* **8**, 2928–2937 (1988).
- Georgopoulos, A. P. Current issues in directional motor control. *Trends Neurosci.* **18**, 506–510 (1995).
- Caminiti, R., Johnson, P. B. & Urbano, A. Making arm movements in different parts of space: dynamic aspects in the primate motor cortex. *J. Neurosci.* **10**, 2039–2058 (1990).
- Moran, D. W. & Schwartz, A. B. Motor cortical representation of speed and direction during reaching. *J. Neurophysiol.* **82**, 2676–2692 (1999).
- Mussa-Ivaldi, F. A. Do neurons in the motor cortex encode movement direction? An alternative hypothesis. *Neurosci. Lett.* **91**, 106–111 (1988).
- Todorov, E. Direct cortical control of muscle activation in voluntary arm movements: a model. *Nature Neurosci.* **3**, 391–398 (2000).
- Kalaska, J. F., Scott, S. H., Cisek, P. & Sergio, L. E. Cortical control of reaching movements. *Curr. Opin. Neurobiol.* **7**, 849–859 (1997).
- Kalaska, J. F., Cohen, D. A. D., Hyde, M. L. & Prud'homme, M. A comparison of movement direction-related versus load direction-related activity in primate motor cortex, using a two-dimensional reaching task. *J. Neurosci.* **9**, 2080–2102 (1989).
- Scott, S. H. & Kalaska, J. F. Reaching movements with similar hand paths but different arm orientations. I. Activity of individual cells in motor cortex. *J. Neurophysiol.* **77**, 826–852 (1997).
- Shen, L. & Alexander, G. E. Preferential representation of instructed target location versus limb trajectory in dorsal premotor area. *J. Neurophysiol.* **77**, 1195–1212 (1997).
- Kakei, S., Hoffman, D. S. & Strick, P. L. Muscle and movement representations in the primary motor cortex. *Science* **285**, 2136–2139 (1999).
- Sanger, T. D. Theoretical considerations for the analysis of population coding in motor cortex. *Neural Comput.* **6**, 12–21 (1994).
- Scott, S. H. & Kalaska, J. F. Motor cortical activity is altered by changes in arm posture for identical hand trajectories. *J. Neurophysiol.* **73**, 2563–2567 (1995).
- Hollerbach, J. M. & Flash, T. Dynamic interactions between limb segments during planar arm movement. *Biol. Cybern.* **44**, 67–77 (1982).
- Mussa-Ivaldi, F. A., Hogan, N. & Bizzi, E. Neural, mechanical, and geometric factors subserving arm posture in humans. *J. Neurosci.* **5**, 2732–2743 (1985).

18. Karst, G. M. & Hasan, Z. Timing and magnitude of electromyographic activity for two-joint arm movements in different directions. *J. Neurophysiol.* **66**, 1594–1604 (1991).
19. Shadmehr, R. & Mussa-Ivaldi, F. A. Adaptive representation of dynamics during learning of a motor task. *J. Neurosci.* **14**, 3208–3224 (1994).
20. Gomi, H. & Kawato, M. Equilibrium-point control hypothesis examined by measured arm-stiffness during multi-joint movement. *Science* **272**, 117–120 (1996).
21. Sainburg, R. L., Ghez, C. & Kalakanis, D. Intersegmental dynamics are controlled by sequential anticipatory, error correction, and postural mechanisms. *J. Neurophysiol.* **81**, 1040–1056 (1999).
22. Scott, S. H., Brown, I. E. & Loeb, G. E. Mechanics of feline soleus: I. Effect of fascicle length and velocity on force output. *J. Muscle Res. Cell Motil.* **17**, 207–219 (1996).
23. Cabel, D. W., Scott, S. H. & Cisek, P. Neural activity in primary motor cortex related to mechanical loads applied to the shoulder and elbow during a postural task. *J. Neurophysiol.* (in the press).
24. Sanger, T. D. Probability density estimation for the interpretation of neural population codes. *J. Neurophysiol.* **76**, 2790–2793 (1996).
25. Zhang, K., Ginzburg, I., McNaughton, B. L. & Sejnowski, T. J. Interpreting neuronal population activity by reconstruction: unified framework with application to hippocampal place cells. *J. Neurophysiol.* **79**, 1017–1044 (1998).
26. Scott, S. H. Apparatus for measuring and perturbing shoulder and elbow joint positions and torques during reaching. *J. Neurosci. Methods* **89**, 119–127 (1999).
27. Gordon, J., Ghilardi, M. F., Cooper, S. E. & Ghez, C. Accuracy of planar reaching movements. II. Systematic extent errors resulting from inertial anisotropy. *Exp. Brain Res.* **99**, 112–130 (1994).
28. Cheng, E. J. & Scott, S. H. Morphometry of *Macaca mulatta* forelimb. I. Shoulder and elbow muscles and segment inertial parameters. *J. Morphol.* **245**, 206–224 (2000).
29. Winter, D. A. Biomechanics of human movement with applications to the study of human locomotion. *Crit. Rev. Biomed. Eng.* **9**, 287–314 (1984).
30. Batschelet, E. *Mathematics in Biology: Circular Statistics in Biology* (Academic, London, 1981).

Supplementary information is available on Nature's World-Wide Web site (<http://www.nature.com>) or as paper copy from the London editorial office of Nature.

**Acknowledgements**

We thank K. Moore for technical assistance and D. Munoz, M. Pare and K. Rose for helpful comments on the manuscript. S. Chan assisted in the training of one monkey. This research was supported by a CIHR grant and scholarship to S.H.S. and a CIHR fellowship to P.L.G.

Correspondence and requests for materials should be addressed to S.H.S. (e-mail: [steve@biomed.queensu.ca](mailto:steve@biomed.queensu.ca)).

**Rae1 and H60 ligands of the NKG2D receptor stimulate tumour immunity**

Andreas Diefenbach, Eric R. Jensen, Amanda M. Jamieson & David H. Raulet

Department of Molecular and Cell Biology and Cancer Research Laboratory, 485 Life Sciences Addition, University of California, Berkeley, California 94720, USA

Natural killer (NK) cells attack many tumour cell lines, and are thought to have a critical role in anti-tumour immunity<sup>1–7</sup>; however, the interaction between NK cells and tumour targets is poorly understood. The stimulatory lectin-like NKG2D receptor<sup>8–13</sup> is expressed by NK cells, activated CD8<sup>+</sup> T cells and by activated macrophages in mice<sup>11</sup>. Several distinct cell-surface ligands that are related to class I major histocompatibility complex molecules have been identified<sup>11–14</sup>, some of which are expressed at high levels by tumour cells but not by normal cells in adults<sup>11,13,15,16</sup>. However, no direct evidence links the expression of these 'induced self' ligands with tumour cell rejection. Here we demonstrate that ectopic expression of the murine NKG2D ligands Rae1 $\beta$  or H60 in several tumour cell lines results in potent rejection of the tumour cells by syngeneic mice. Rejection is mediated by NK cells and/or CD8<sup>+</sup> T cells. The ligand-expressing tumour cells induce potent priming of cytotoxic T cells and sensitization of NK cells *in vivo*. Mice that are exposed to live or irradiated tumour cells expressing Rae1 or H60 are specifically immune to subsequent challenge with tumour cells that lack NKG2D ligands, suggesting application of the ligands in the design of tumour vaccines.

As demonstrated by staining with a tetramerized derivative of the extracellular portion of NKG2D, NKG2D ligands are expressed by most of the tumour cells tested, including various lymphoid, myeloid and carcinoma cell lines (ref. 11; and A. Diefenbach and D. Raulet, unpublished data). Northern blot analysis showed that many of the positive cell lines express Rae1 transcripts, whereas H60 transcripts were limited to only one or two of the cell lines tested (data not shown). Rae1 transcripts have not been detected in normal cells from adult mice<sup>15</sup>, suggesting that these genes are specifically upregulated in tumour cell lines.

To investigate whether tumour cells that express NKG2D ligands stimulate anti-tumour immune responses, we used a retrovirus expression system to ectopically express high levels of Rae1 $\beta$  or H60 in EL4 (a thymoma), RMA (a T-cell lymphoma) and B16-BL6 (a melanoma). These cell lines are all from C57BL/6 (hereafter termed B6) mice and do not normally express NKG2D ligands<sup>11</sup>. Ligand-transduced cells were selected on the basis of staining with NKG2D tetramers. To serve as controls, tumour cells that were transduced with empty retrovirus vector (designated as EL4<sup>-</sup>, B16<sup>-</sup> and RMA<sup>-</sup>) were selected by genomic polymerase chain reaction (PCR) (see Methods).

For analysis of the response to EL4 and B16-BL6 tumour cells, groups of five B6 mice were inoculated subcutaneously with syngeneic tumour cell transductants. Control-transduced EL4 or B16-BL6 cells grew progressively at a rate similar to that of untransduced cells (Fig. 1a, c, d, and data not shown), leading to uniform terminal morbidity by about 28 days. Notably, Rae1 $\beta$ - or H60-transduced tumour cells of both types were rejected rapidly and completely, as they failed to yield detectable tumours at any time point (Fig. 1a, c, d). A tenfold increase in the dose of Rae1 $\beta$ - or H60-transduced EL4 cells (to  $5 \times 10^7$  cells) did not change the outcome, whereas a higher dose ( $1 \times 10^5$ ) of Rae1 $\beta$ - or H60-transduced B16-BL6 cells resulted in progressive, although substantially delayed, tumour growth in all the mice, compared with the control-transduced tumour cells (data not shown). Ligand-transduced tumour cells of both types also failed to grow in B6 mice that had been depleted of CD8<sup>+</sup> T cells or in B6-Rag1<sup>-/-</sup> mice—which lack all T and B cells—but grew progressively in normal and B6-Rag1<sup>-/-</sup> hosts that had been depleted of NK1.1<sup>+</sup> cells (Fig. 1a–e). Thus, these doses of Rae1 $\beta$ - or H60-transduced EL4 cells and B16-BL6 cells are rejected rapidly by conventional NK cells without a requirement for T and B cells, including NK1.1<sup>+</sup> T cells or  $\gamma\delta$  T cells. Interestingly, Rae1 $\beta$ - or H60-transduced B16-BL6 cells reproducibly exhibited retarded growth in NK-depleted B6-Rag1<sup>-/-</sup> mice (Fig. 1e). It is possible that a residual response against these cells is mediated by non-lymphoid cells such as macrophages, or by small numbers of NK cells that survive antibody treatment.

Rae1 $\beta$  or H60 expression by B16-BL6 cells reduced the frequency of lung metastases by over tenfold after intravenous injection (Fig. 1f). In another experiment where mice were examined at a later time point, control-transduced B16-BL6 cells formed massive contiguous lung metastases, but ligand-transduced B16-BL6 cells were almost completely rejected (Fig. 1g). NK1.1 depletion before tumour cell inoculation markedly depressed the rejection of the metastases.

Rae1 $\beta$ - or H60-transduced RMA tumour cells were also rejected by B6 mice (Fig. 2). Unlike the responses to the other tumour cells, however, the primary rejection of ligand-transduced RMA cells was mediated by both CD8<sup>+</sup> T cells and NK cells, although the specific outcome depended on the dose of tumour cells. Depletion of both NK1.1<sup>+</sup> cells and CD8<sup>+</sup> T cells was necessary to abrogate rejection of the smallest inoculum of  $10^4$  ligand-transduced tumour cells, whereas depletion of either population allowed tumour growth in at least some animals that were injected with the largest dose ( $10^6$ ) of tumour cells (Fig. 2a). With the intermediate dose of  $10^5$  tumour cells, depletion of CD8 cells allowed tumour cell growth, but NK cell depletion did not (Fig. 2a). Thus, either subset is sufficient for